SUPPLEMENTARY MATERIAL

Study of the electrochemical oxidation of 4,6-dimethyldibenzothiophene on a BDD electrode employing different techniques

O. Ornelas Dávila[a], L. Lacalle Bergeron[b], P. Ruiz Gutiérrez[c], M. M. Dávila Jiménez[a,*], I. Sirés[d], E. Brillas[d], A.F. Roig Navarro[b], J. Beltrán Arandes[b], J.V. Sancho Llopis[b]

[a] *Facultad de Ciencias Químicas, Benemérita Universidad Autónoma de Puebla, Mexico*

[b] *Instituto Universitario de Plaguicidas y Aguas (IUPA), Universidad Jaume I, Castellón de la Plana, Spain*

[c] *Centro de Química Instituto de Ciencias, Benemérita Universidad Autónoma de Puebla, Mexico*

[d] *Laboratori d'Electroquímica dels Materials i del Medi Ambient, Departament de Química Física, Facultat de Química, Universitat de Barcelona, Martí i Franquès 1-11, 08028 Barcelona, Spain*

* Corresponding author, E-mail: mdavila.uap.mx@gmail.com

Text S1

HPLC-UV analysis

The electrolyzed solutions were collected at different electrolysis times, and the HPLC-UV analysis to monitor the abatement of 4,6-DMDBT concentration during its oxidation upon bulk electrolysis was performed using a 1260 Infinity Series Instrument LC-DAD chromatograph coupled to a 1260 Infinity Multiple Detector (MWD) from Agilent Technologies, (Santa Clara, CA). A Kinetex Reversed Phase C18 100 Å (30 mm × 2.1 mm) column at 28 ºC was utilized with a gradient elution at 0.5 mL min^{-1} programmed as follows: acetonitrile-water (10% A-90% B) for 0-14 min, 90% B at 14-20 min and (90% A-10% B) at 20-25 min. Both solvents contained 0.1% formic acid (reagent grade purchased from Sigma-Aldrich). The injection volume was 5 μL and the detection wavelengths were 208, 232, 244 and 254 nm.

Text S2

GC-MS analysis

After evaporation, the solid phase was dissolved in methanol to analyze the oxidized products using a Varian CP-3800 gas chromatograph coupled to a mass spectrometry detector (Saturn 4000, Varian). The compounds were separated on an HP-5 (30 m × 0.25 mm, 0.25 μm film thickness) capillary column, using helium as carrier gas at a constant flow rate of 1 mL min^{-1}. The temperature program was: 70 °C for 2 min, up to 150 °C at 30 °C min^{-1} and then, up to 250 °C at 5 °C min^{-1}, with a final isothermal stage for 25.33 min. A 100 μL sample was injected in splitless mode (injection port temperature of 220 °C) using a Varian 8400 autosampler equipped with a 10 μL syringe. Ion trap MS determination was carried out in full scan mode (*m/z* scan range of 40-600 Da) using EI ionization at 70 eV in positive mode and external ionization configuration. GC-MS interface, ion trap and manifold temperatures were 275, 190 and 60 °C, respectively.

Text S3

UHPLC-ESI-Q-TOF-MS analysis

The electrolyzed solutions were concentrated by evaporation. Then, they were diluted (1:100) for the analysis of the products by UHPLC-ESI-Q-TOF-MS. The modern Q-TOF-MS instruments allow the simultaneous acquisition of two full spectra with different collision energies in a single injection (MSE mode). The use of the low energy (LE) function with a collision energy of 4 eV informs about non-fragmented ions related to the parent protonated molecule $[M+H]^+$ in positive ionization mode. The high energy (HE) function, with a collision energy ramp ranging from 15 to 40 eV, provides a wide range of fragmented ions.

A Waters Acquity ultra-performance liquid chromatography (UPLC) system (Waters, Milford) was employed. The separation was performed using an Acquity UPLC BEH C18 (2.1 mm × 100 mm, 1.7 μm particle size) column from Waters. The mobile phases contained water (A) and/or methanol (B), both with 0.01% formic acid. The percentage of B changed as follows: 10% at 0 min, 90% at 14 min, and 10% again at 16.10 min. The flow rate was 300 μL min^{-1} and the analysis run time was 18 min. The sample injection volume was 20 μL. The UPLC system was interfaced to a hybrid quadrupole-TOF high resolution mass spectrometer (HRMS) (Xevo G2 Q-TOF, Waters Micromass), using an orthogonal Z-spray-ESI interface operating in both positive and negative ion mode. TOF-MS resolution was approximately 25000 at full width-half maximum at *m/z* 556. Nitrogen was used as drying and nebulizing gas at a flow rate of 800 $L \cdot h^{-1}$. The MS data were acquired over an *m/z* range of 50-1200 at a scan time of 0.4 s. A capillary voltage of 0.7 kV and cone voltage of 20 V were used in positive ionization mode. The collision gas was argon (99.995%, Praxair). The interface, source and column temperatures were 450, 150 and 40 ºC, respectively.

Text S4

ICP-MS analysis

Qualitative determination of niobium in electrolyzed solutions was conducted with an Agilent 7500cx ICP-MS instrument. For this purpose, the selected samples were evaporated to dryness and redissolved with 2 mL of 1% HNO_3. Afterwards, the resulting samples were nebulized to the ICP-MS and the signal at *m/z* 93 was monitored in qualitative mode (20 points per peak). Reagents free of Nb were checked from the analysis of blank solutions with 1% HNO_3.

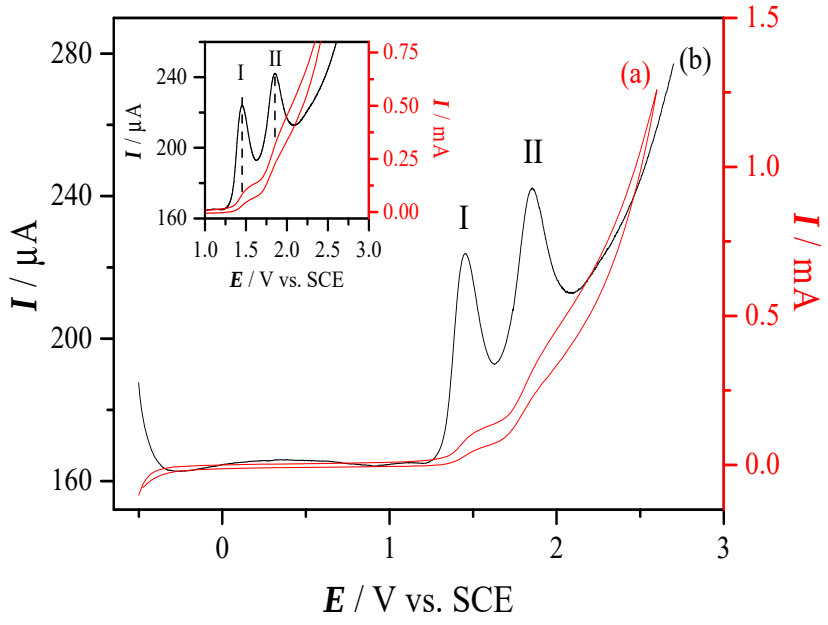

Fig. S1. (a) CV and (b) DPV curves obtained with 14 mg L^{-1} 4,6-DMDBT in ACN (93.5% v/v)–water (6.5% v/v, 0.010 M $LiClO_4$) using a BDD electrode at ν = 0.005 V s^{-1}.

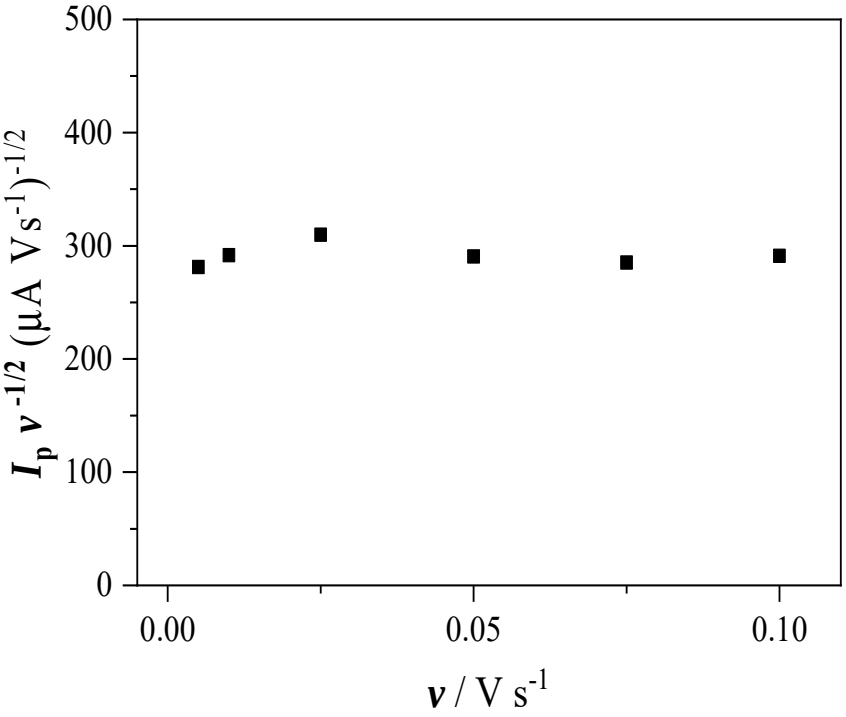

Fig. S2. Variation of ($I_p\, v^{-1/2}$) vs. scan rate for peak I recorded by CV, as shown in Fig. 3a.

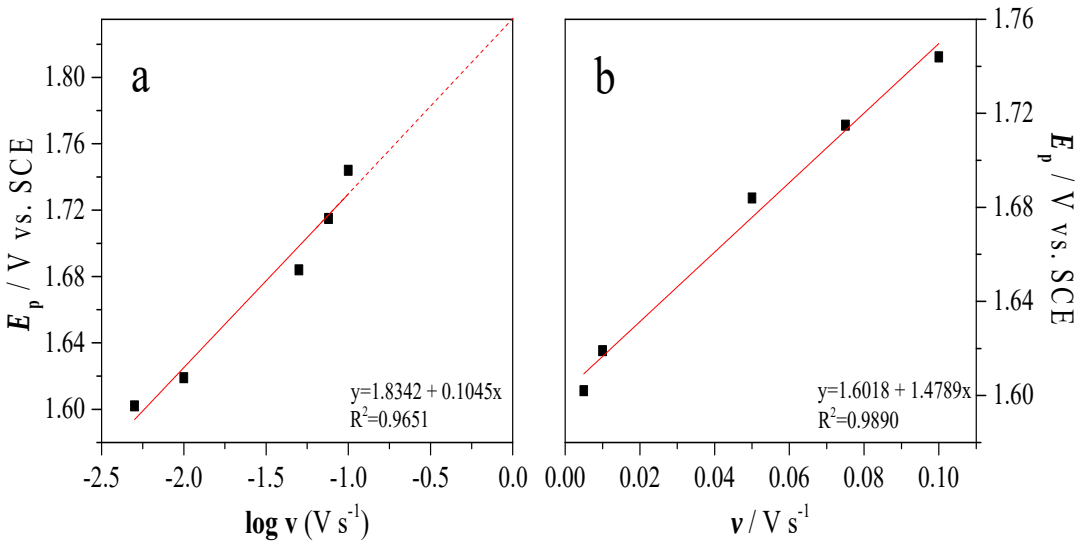

78

79 **Fig. S3.** Variation of the peak potential with the (a) logarithm of scan rate and (b) scan rate,

80 corresponding to the oxidation peak found in the cyclic voltammograms of Fig. 3a.

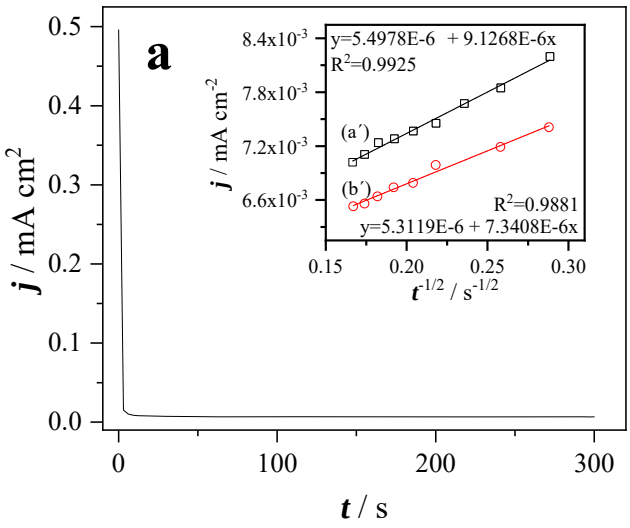

81

82 Fig. S4. (a) Chronoamperogram obtained with BDD in the presence of 27 mg L^{-1} 4,6-

83 DMDBT in ACN (93.5% v/v)–water (6.5% v/v, 0.010 M $LiClO_4$) solution at 1.5 V. Inset:

84 Cottrell plot obtained from the chronoamperogram in the presence of (a′) 27 mg L^{-1} and (b′)

85 14 mg L^{-1} of 4,6-DMDBT.

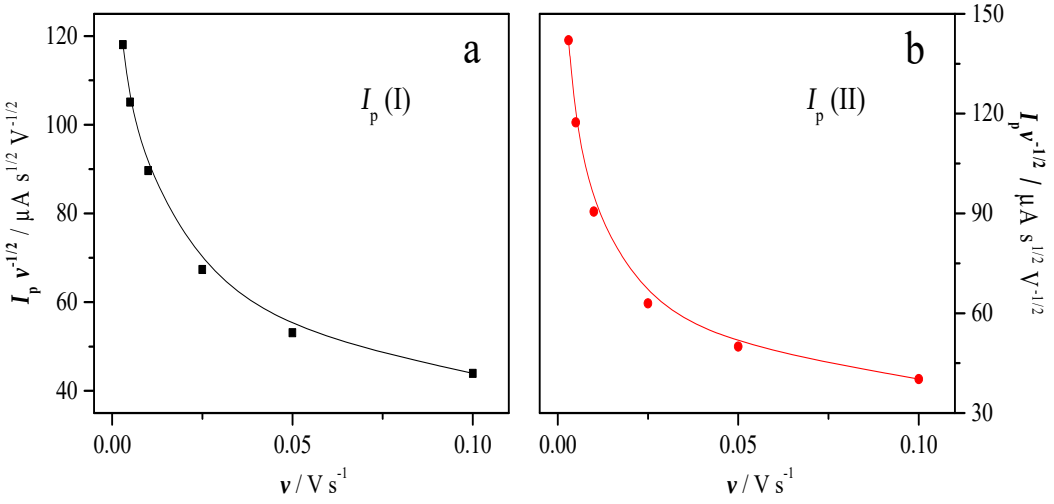

86

87 **Fig. S5.** Change of (I_p $v^{-1/2}$) with scan rate for peaks (a) I and (b) II recorded by DPV, as

88 shown in Fig. 4a.

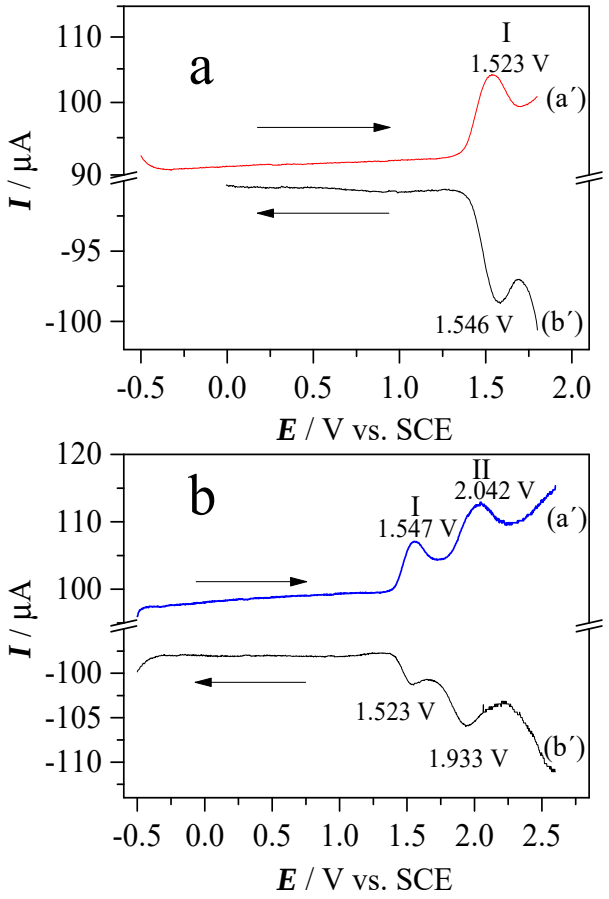

Fig. S6. DPV curves obtained with 14 mg L^{-1} 4,6-DMDBT in ACN (93.5% v/v)–water (6.5% v/v, 0.010 M $LiClO_4$) using a BDD electrode. (a) Potential range from -0.50 to +1.75 V for the (a') anodic and (b') cathodic scans at v = 0.003 V s^{-1}. (b) Potential range from -0.50 to +2.60 V for the (a') anodic and (b') cathodic scans at v = 0.003 V s^{-1}.

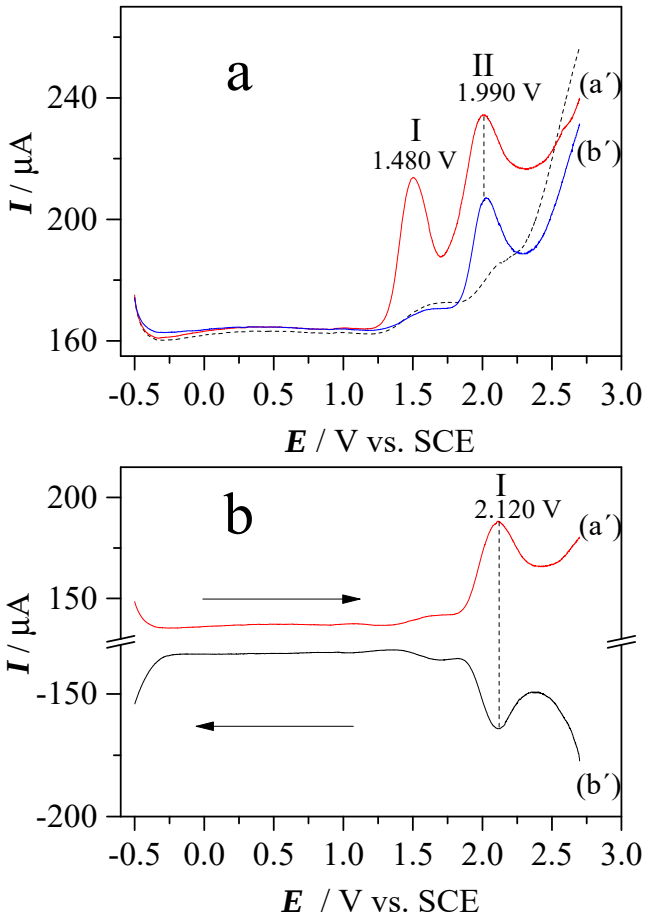

94

95 **Fig. S7.** (a) DPV profiles recorded during oxidation scan in (---) ACN (93.5% v/v)–water
96 (6.5% v/v, 0.010 M $LiClO_4$) using a BDD electrode at $v = 0.003$ V s^{-1}, and in the presence of
97 27 mg L^{-1} of (a') DBT and (b') $DBTO_2$. (b) DPV curves obtained with 27 mg L^{-1} $DBTO_2$ in
98 the potential range from -0.50 to +2.75 V for the (a') anodic and (b') cathodic scans.

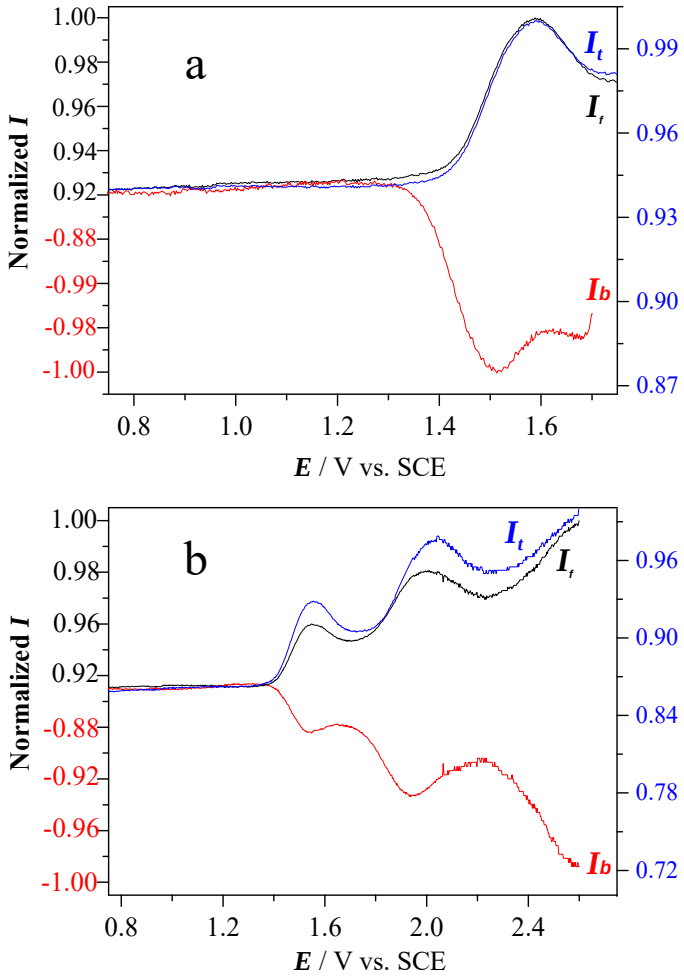

Fig. S8. SWV curves determined with 14 mg L^{-1} 4,6-DMDBT in ACN (93.5% v/v)–water (6.5% v/v, 0.010 M $LiClO_4$) using a BDD electrode at a frequency of 8 Hz and v = 0.020 V s^{-1}. Potential range: (a) from -0.50 to +1.80 V and (b) from -0.50 to +2.60 V. Current in the anodic (forward) scan: I_f; current in the cathodic (backward) scan: I_b; total current: I_t.

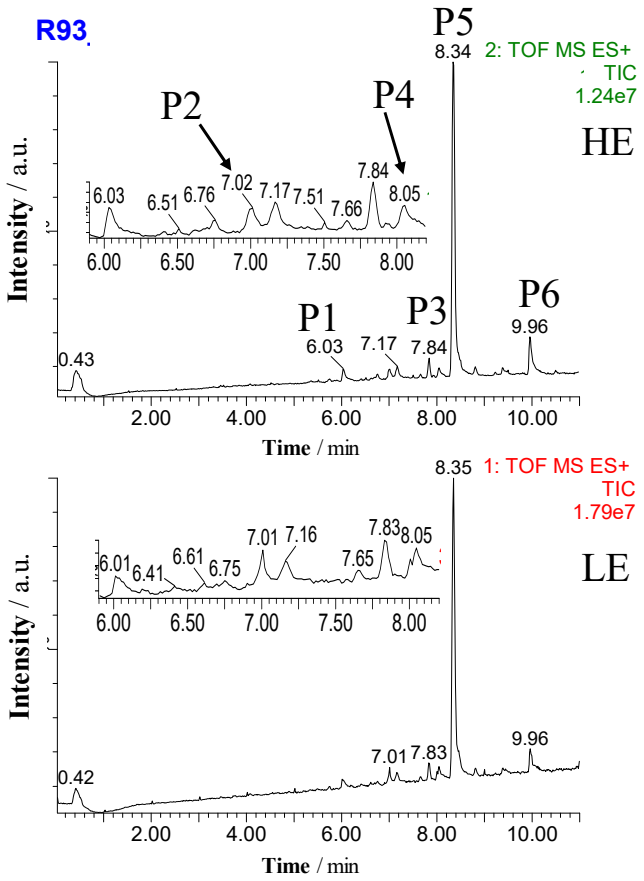

104

105 **Fig. S9.** Total ion chromatograms obtained from the UHPLC-ESI-Q-TOF-MS analysis of
106 samples collected after electrolysis of 27 mg L^{-1} 4,6-DMDBT in ACN (93.5% v/v)–water
107 (6.5% v/v, 0.010 M $LiClO_4$) for 90 min in a BDD/BDD cell at 1.50 V. High energy (HE) and
108 low energy (LE).

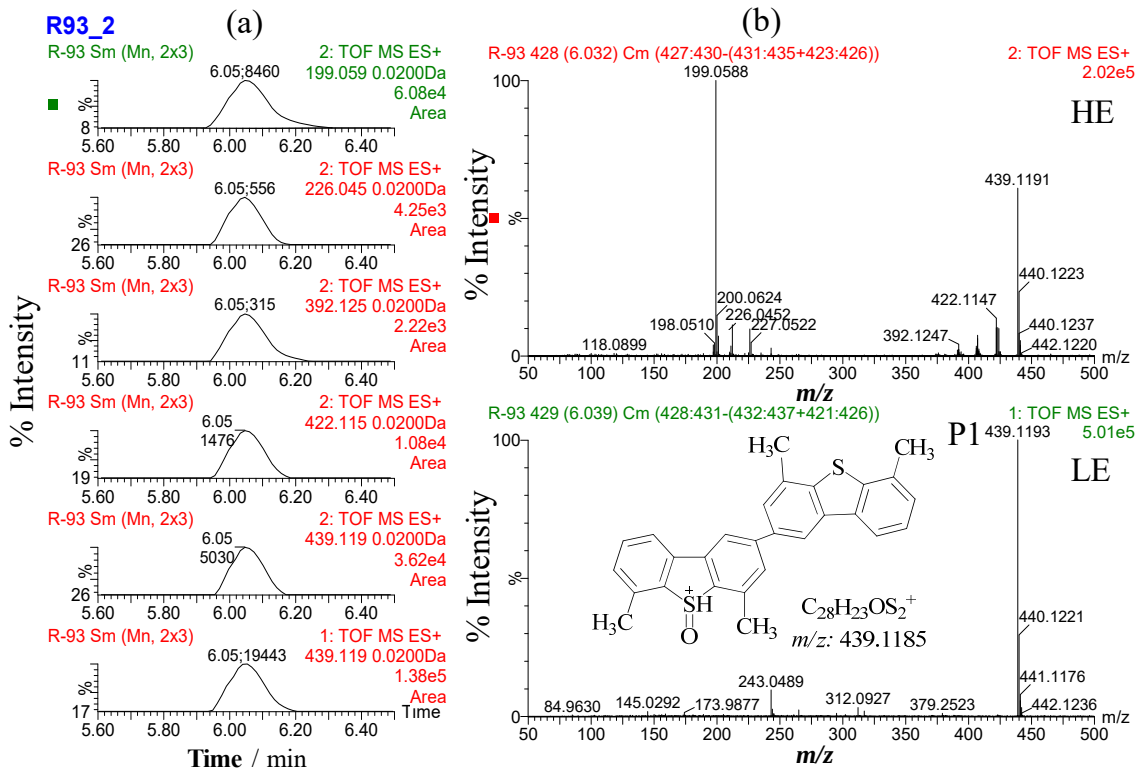

Fig. S10. Detection and identification of compounds with possible chemical structure: $C_{28}H_{22}OS_2$ in the extracts obtained upon electrolysis of 27 mg L^{-1} 4,6-DMDBT at 1.5 V for 90 min. LE and HE TOF mass spectra for the sample (b) and extracted ion chromatograms (XICs) at 20 mDa mass window (a) for $[M+H]^+$ in LE function and main fragments in HE function. Possible structure assigned by Mass Fragment software.

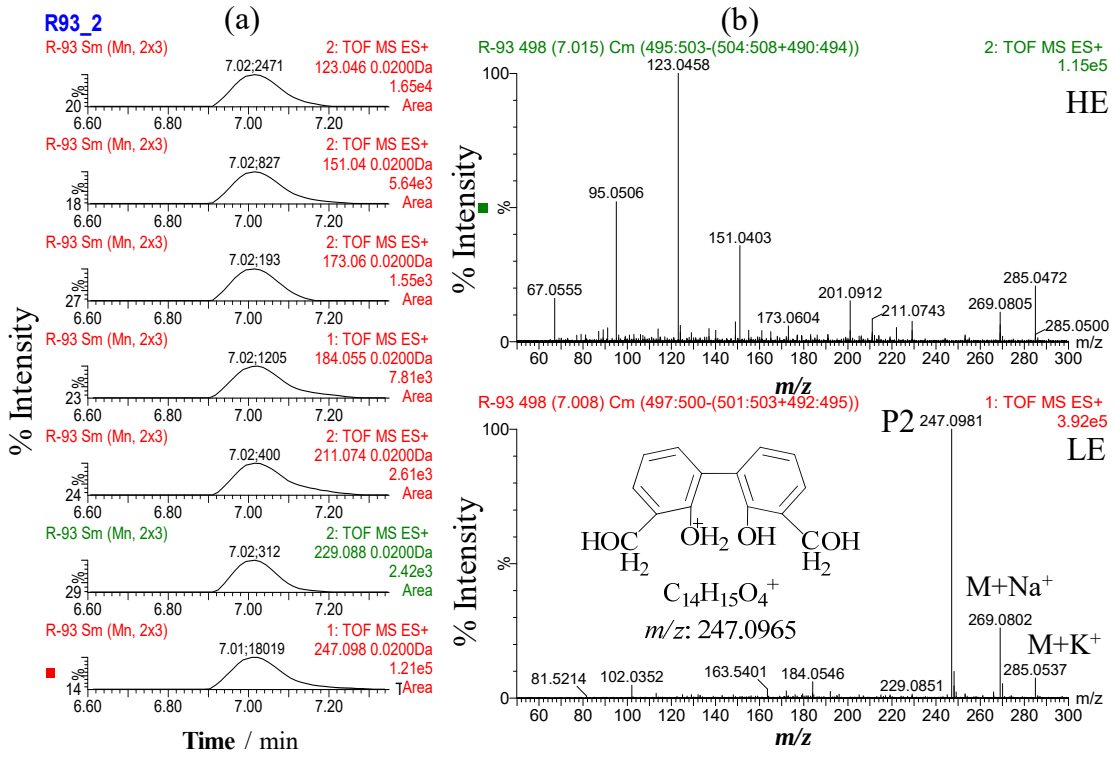

115

116 **Fig. S11.** Detection and identification of compounds with possible chemical structure:
117 $C_{14}H_{14}O_4$ in extracts obtained upon electrolysis of 27 mg L^{-1} 4,6-DMDBT at 1.5 V for 90
118 min. The LE and HE TOF mass spectra for (a) and (b), as well as the possible structure
119 assigned, were obtained upon the same conditions of Fig. S10.

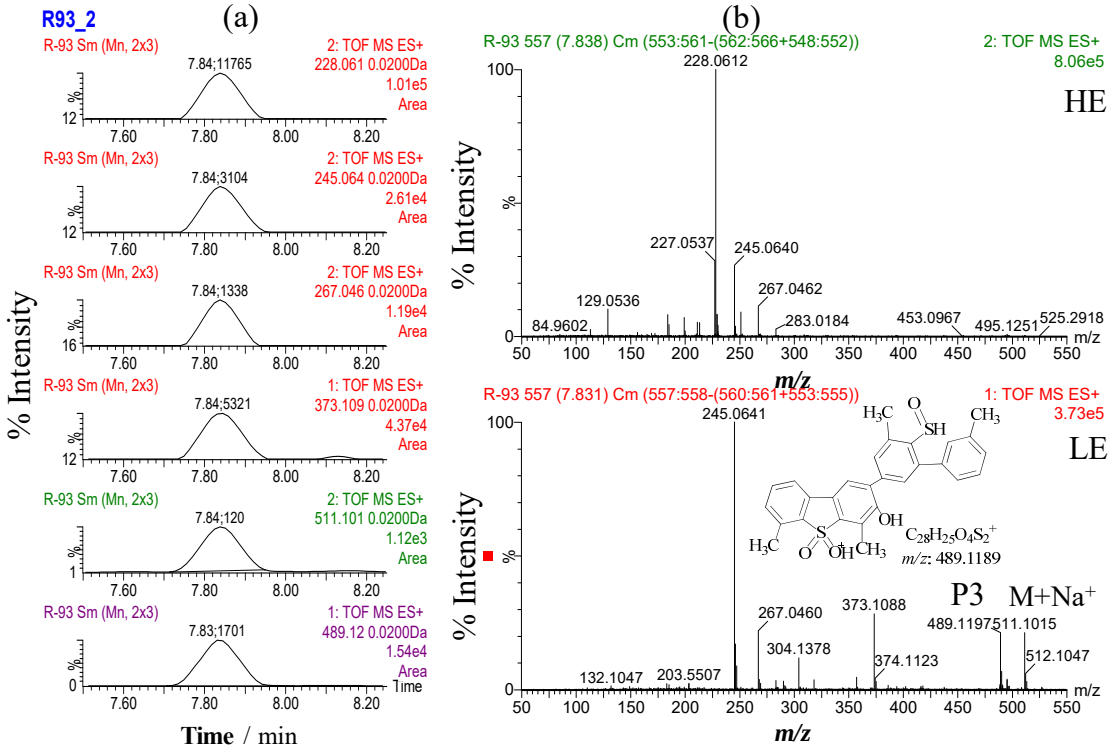

120

121 **Fig. S12.** Detection and identification of compounds with possible chemical structure:
122 $C_{28}H_{24}O_4S_2$ in extracts obtained upon electrolysis of 27 mg L^{-1} 4,6-DMDBT at 1.5 V for 90
123 min. The LE and HE TOF mass spectra for (a) and (b), as well as the possible structure
124 assigned, were obtained upon the same conditions of Fig. S10.

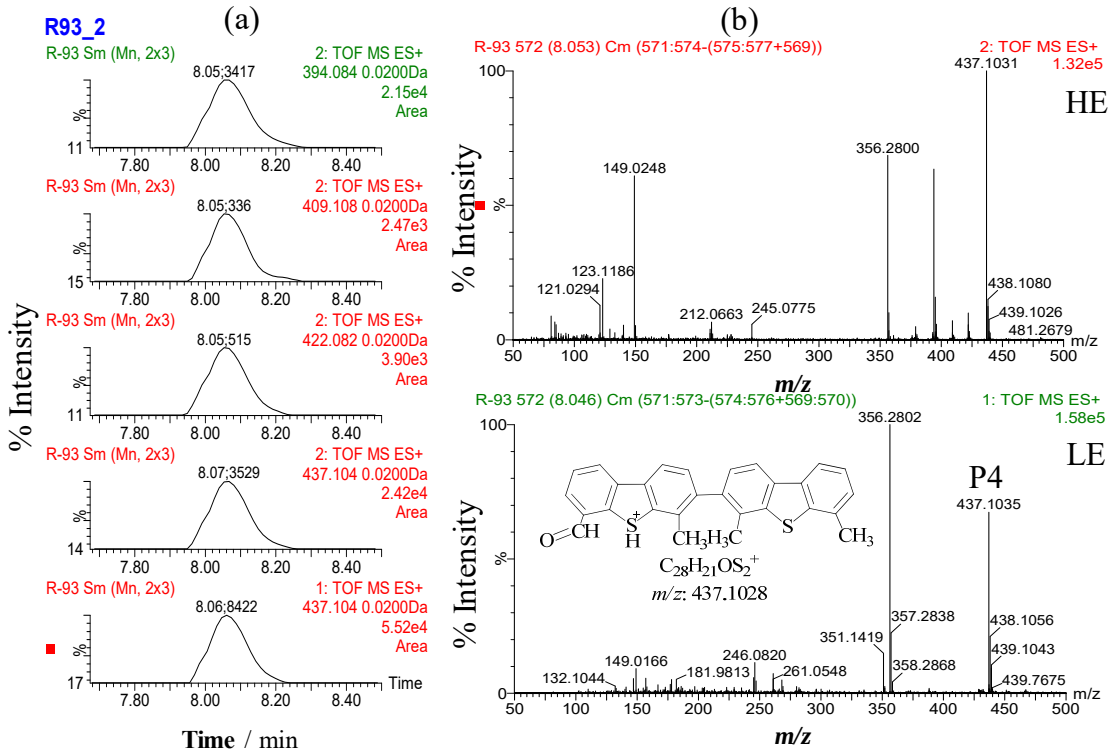

125

126 **Fig. S13.** Detection and identification of compounds with possible chemical structure:
127 $C_{28}H_{20}OS_2$ in extracts obtained upon electrolysis of 27 mg L^{-1} 4,6-DMDBT at 1.5 V for 90
128 min. The LE and HE TOF mass spectra for (a) and (b), as well as the possible structure
129 assigned, were obtained upon the same conditions of Fig. S10.

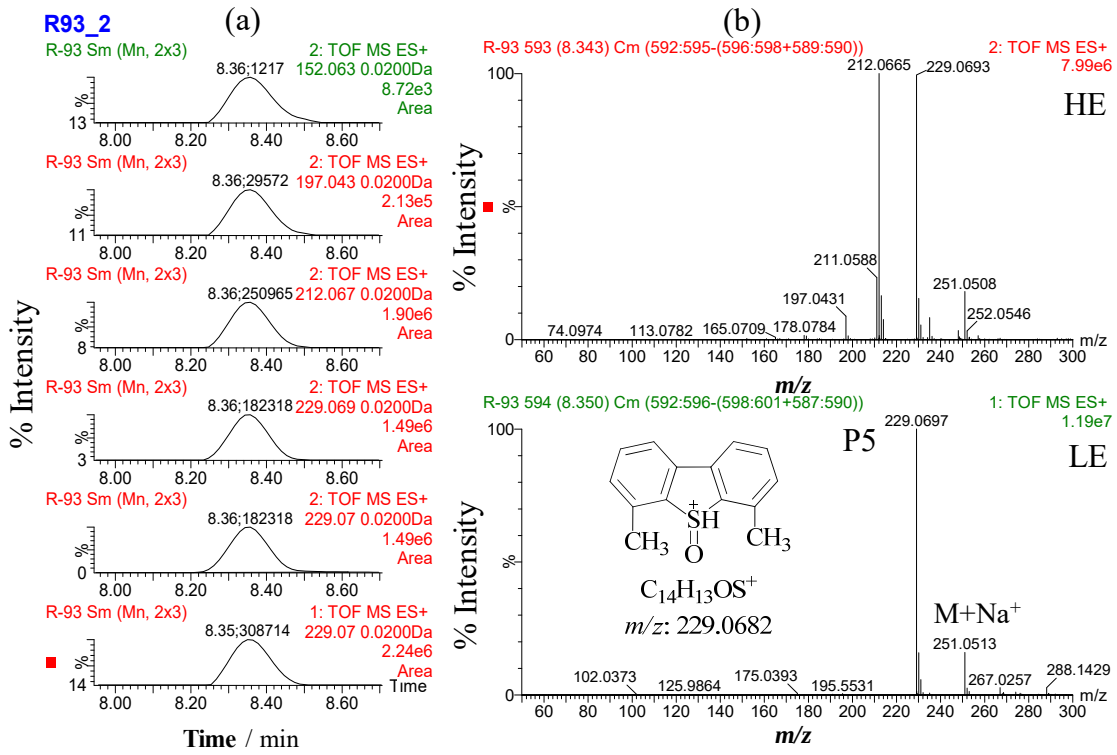

130

131 **Fig. S14.** Detection and identification of compounds with possible chemical structure:
132 $C_{14}H_{12}OS$ in extracts obtained upon electrolysis of 27 mg L^{-1} 4,6-DMDBT at 1.5 V for 90
133 min. The LE and HE TOF mass spectra for (a) and (b), as well as the possible structure
134 assigned, were obtained upon the same conditions of Fig. S10.

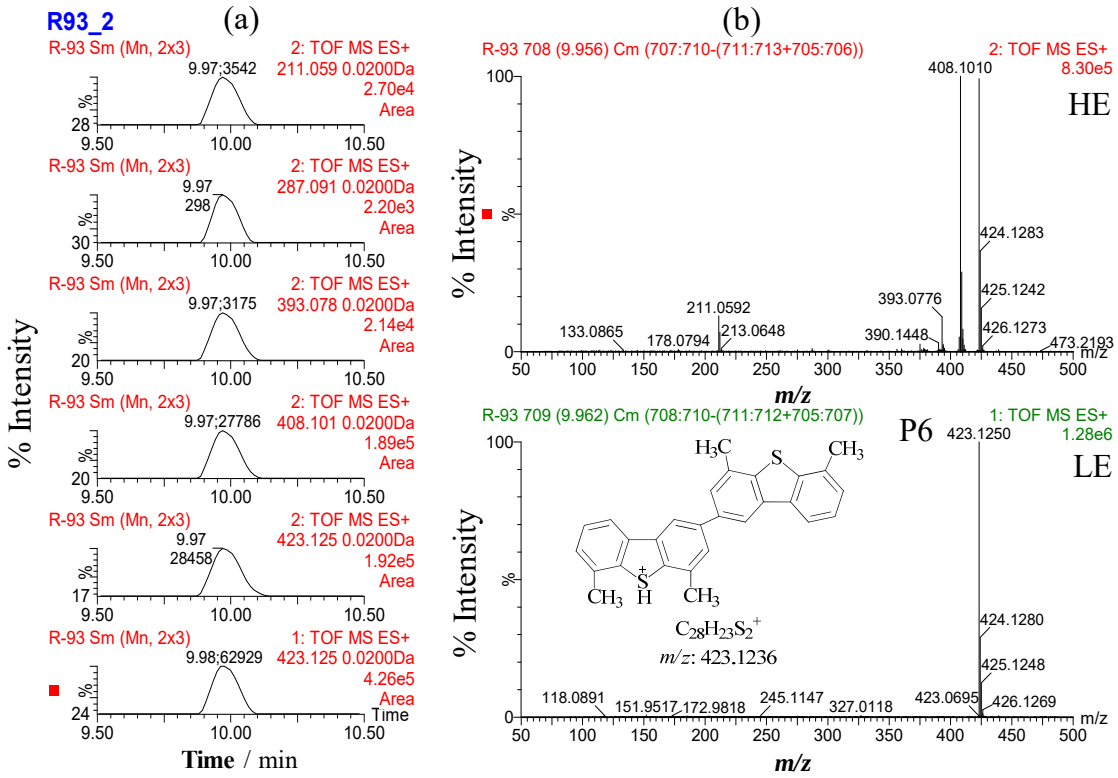

135

136 **Fig. S15**. Detection and identification of compounds with possible chemical structure:
137 $C_{28}H_{22}S_2$ in extracts obtained upon electrolysis of 27 mg L^{-1} 4,6-DMDBT at 1.5 V for 90
138 min. The LE and HE TOF mass spectra for (a) and (b), as well as the possible structure
139 assigned, were obtained upon the same conditions of Fig. S10.

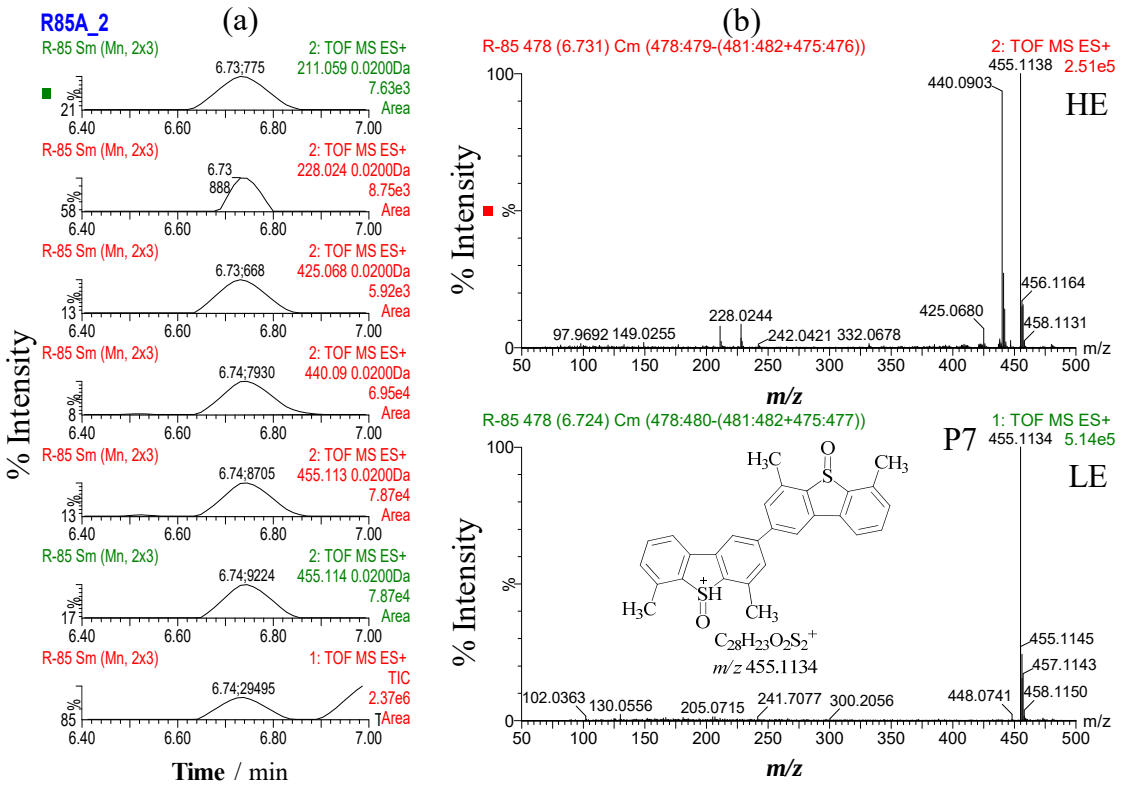

140

141 **Fig. S16**. Detection and identification of compounds with possible chemical structure:

142 $C_{28}H_{22}O_2S_2$ in extracts obtained upon electrolysis of 27 mg L^{-1} 4,6-DMDBT at 1.5 V for 90

143 min. The LE and HE TOF mass spectra for (a) and (b), as well as the possible structure

144 assigned, were obtained upon the same conditions of Fig. S10.

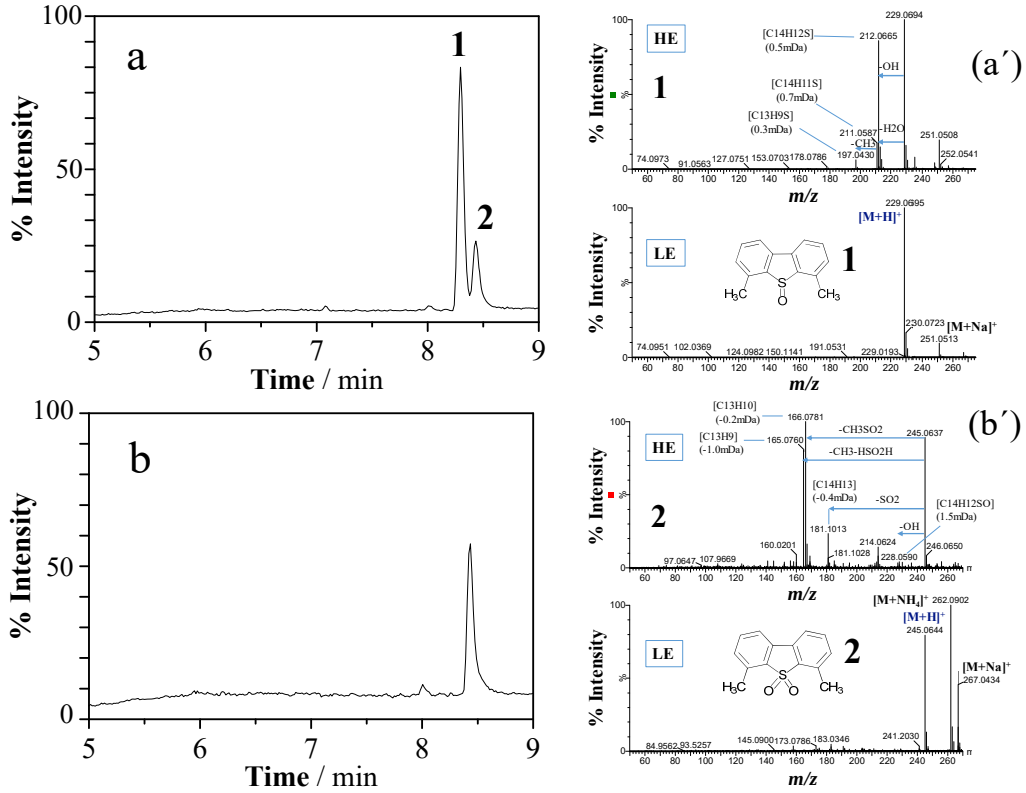

145

146 **Fig. S17.** Total ion chromatograms obtained from the UHPLC-ESI-Q-TOF-MS analysis of
147 samples collected after electrolysis of 27 mg L^{-1} 4,6-DMDBT in ACN (93.5% v/v)–water
148 (6.5% v/v, 0.010 M $LiClO_4$) for 240 min in a BDD/BDD cell, at (a) 1.50 and (b) 2.00 V. HE
149 and LE mass spectra for (a') 4,6-DMDBTO at retention time of 8.30 min (compound 1) and
150 (b') 4,6-$DMDBTO_2$ at retention time of 8.43 min (compound 2).

Table S1. Products, t_R and ESI-TOF-MS mass spectral properties of fragments formed from bulk electrolysis carried out for 90 min at E_{an} = 1.5 V.

Peak	t_R (min)	Experimental mass (*m/z*)	mDa	Elemental composition	Fragments (*m/z*)	mDa	Lost fragments
P1	6.04	439.1191	0.1	$C_{28}H_{23}OS_2^+$			
					422.1147	-1.6	OH
					392.1247	1.2	CH_3
					226.0452	0.0	$C_{14}H_{13}S$
					199.0588	0.7	$C_{15}H_{12}OS$
P2	7.01	247.0982	1.2	$C_{14}H_{15}O_4^+$			
					229.0865	-1.0	H_2O
					211.0793	-1.3	$2H_2O$
					184.0546	2.2	$C_2H_7O_2$
					173.0606	0.3	$C_4H_6O_2$
					151.0404	0.9	C_6H_8O
					123.0458	1.2	$C_7H_8O_2$
P3	7.83	489.1197	0.3	$C_{28}H_{25}O_4S_2^+$			
					373.1088	0.3	$C_4H_4O_4$
					267.0462	-1.8	$C_{12}H_{14}O_2S$
					245.0640	0.4	$C_{14}H_{12}O_2S$
					228.0612	0.3	$C_{14}H_{13}O_3S$
P4	8.04	437.1031	-0.3	$C_{28}H_{21}OS_2^+$			
					422.0816	-0.8	CH_3
					409.1082	1.7	CO
					394.0845	-0.5	C_2H_3O
P5	8.35	229.0693	0.6	$C_{14}H_{13}OS^+$			
					212.0665	0.5	OH
					197.0431	0.6	CH_4O
					178.0783	0.0	H_3OS
					152.0628	0.2	C_2H_5OS
P6	9.96	423.1248	0.7	$C_{28}H_{23}S_2^+$			
					408.1010	0.4	CH_3
					393.0776	0.4	$2CH_3$
					287.0911	1.7	C_8H_8S
					211.0592	1.1	$C_{10}H_{12}S$
					178.0796	1.3	$C_{14}H_{13}S2$
*P7	6.74	455.1138	-0.1	$C_{28}H_{23}O_2S_2^+$			
					440.0905	-0.2	CH_3
					425.0680	1.0	$2CH_3$
					228.0244	-	$C_{14}H_{11}OS$
					211.0588	0.7	$C_{14}H_{12}O_2S$

* P7 Product obtained for long electrolysis time of 240 min